ARTICLE

Defining the Cause of Skewed X-Chromosome Inactivation in X-Linked Mental Retardation by Use of a Mouse Model

Mary R. Muers, Jacqueline A. Sharpe, David Garrick, Jacqueline Sloane-Stanley, Patrick M. Nolan, Terry Hacker, William G. Wood, Douglas R. Higgs, and Richard J. Gibbons

Extreme skewing of X-chromosome inactivation (XCI) is rare in the normal female population but is observed frequently in carriers of some X-linked mutations. Recently, it has been shown that various forms of X-linked mental retardation (XLMR) have a strong association with skewed XCI in female carriers, but the mechanisms underlying this skewing are unknown. ATR-X syndrome, caused by mutations in a ubiquitously expressed, chromatin-associated protein, provides a clear example of XLMR in which phenotypically normal female carriers virtually all have highly skewed XCI biased against the X chromosome that harbors the mutant allele. Here, we have used a mouse model to understand the processes causing skewed XCI. In female mice heterozygous for a null *Atrx* allele, we found that XCI is balanced early in embryogenesis but becomes skewed over the course of development, because of selection favoring cells expressing the wild-type *Atrx* allele. Unexpectedly, selection does not appear to be the result of general cellular-viability defects in Atrx-deficient cells, since it is restricted to specific stages of development and is not ongoing throughout the life of the animal. Instead, there is evidence that selection results from independent tissue-specific effects. This illustrates an important mechanism by which skewed XCI may occur in carriers of XLMR and provides insight into the normal role of ATRX in regulating cell fate.

X-chromosome inactivation (XCI) is the mechanism by which gene dosage equivalence is achieved between female (XX) and male (XY) mammals.[1] XCI occurs in individual cells early in embryonic development and is subsequently stably maintained in all daughter cells. Therefore, each tissue of an adult female is composed of cells that express either the maternal or the paternal X chromosome. Because which X chromosome will be silenced is random, in the general female population, XCI ratios have a normal distribution, with an average of ~50:50, so that an equal number of cells express the maternal and paternal chromosomes.[2] Therefore, by chance, a small percentage of females (~9%) have a skewed ratio (>80:20), where there is a bias toward cells expressing one or the other X chromosome, but extreme skewing (>95:5) is very rare (in <1% of females).[2]

Whereas skewed XCI is rare in the normal population, it is relatively common in carriers of X-linked mutations and in cases of X-autosome translocations. In principle, heterozygosity for an X-linked mutation could cause skewed XCI, either by biasing the primary pattern of XCI (as is the case for the *Xce* locus in mice[3–6]) or through secondary selection in favor of cells expressing a particular X chromosome.[7–9] When skewed XCI is limited to specific tissues,[10,11] it can be assumed that this is because of cell selection, but, when XCI is skewed to a similar extent in many or all tissues, although this could result from cell selection due to a defect in a basic cellular function, this is not necessarily the case.

Recently, it has been shown that several X-linked mental retardation (XLMR) disorders have a strong association with skewed XCI in carrier females.[12] However, the mechanism underlying skewing in these cases is unknown. A clear example of this association is seen in the α-thalassemia XLMR syndrome (ATR-X syndrome [MIM 301040]). Affected males have profound psychomotor retardation and multiple congenital abnormalities, including facial dysmorphism and urogenital and skeletal defects.[13–15] ATR-X syndrome was originally identified via the unusual association of mental retardation with mild α-thalassemia, characterized by the formation of HbH inclusions (β-globin tetramers) in red blood cells.[16] ATRX is a ubiquitously expressed, chromatin-associated protein of the Snf2 family and is thought to affect the expression of α-globin and a wide range of other genes via epigenetic mechanisms.[17–22]

Nearly all female carriers of ATR-X syndrome have highly skewed XCI in favor of cells expressing the normal *ATRX* allele and are essentially phenotypically normal.[23] In some carriers, a few red cells (~1% of the frequency seen in affected males) contain HbH inclusions. In a unique carrier female with balanced XCI in the peripheral blood, the percentage of HbH cells (0.9%) was similar to that seen in affected males, consistent with skewed XCI being the mechanism by which such carriers are normally

From the Medical Research Council (MRC) Molecular Haematology Unit, Weatherall Institute of Molecular Medicine, John Radcliffe Hospital, Oxford, United Kingdom (M.R.M.; J.A.S.; D.G.; J.S.-S.; W.G.W.; D.R.H.; R.J.G.); and MRC Mammalian Genetics Unit, Didcot, Oxfordshire, United Kingdom (P.M.N.; T.H.)

Received January 16, 2007; accepted for publication March 22, 2007; electronically published April 25, 2007.

Address for correspondence and reprints: Dr. Richard Gibbons, MRC Molecular Haematology Unit, Weatherall Institute of Molecular Medicine, John Radcliffe Hospital, Oxford, OX3 9DS, United Kingdom. E-mail: richard.gibbons@imm.ox.ac.uk

Am. J. Hum. Genet. 2007;80:1138–1149. 0002-9297/2007/8006-0013$15.00
DOI: 10.1086/518369

protected from the deleterious effects of an *ATRX* mutation.[23]

Like *ATRX,* many XLMR genes are widely expressed and are predicted to regulate general nuclear processes, such as transcription, DNA repair, and cell proliferation.[24] Therefore, it has been proposed that mutations in such genes should result in general defects influencing cell viability or proliferation and thus should result in skewed XCI (due to cell selection) in a wide variety of cell types.[12] Although most analyses of XCI in XLMR have been performed on peripheral blood, in ATR-X syndrome, skewed XCI has been demonstrated in buccal cells, hair roots, and peripheral blood (originating from endoderm, ectoderm, and mesoderm, respectively). As originally proposed,[23] this could result from cell selection prior to the differentiation of the embryo into separate tissue types, from separate selection events in different tissues, or from an effect of the mutation on the primary establishment of XCI. Which of these actually occurs in vivo has not yet been demonstrated for any form of XLMR in which carrier females have skewed XCI.

Here, we have examined the pattern of XCI in female mice heterozygous for a null mutation in the highly conserved mouse orthologue of *ATRX* (*Atrx* [GenBank accession number NM_009530]).[25,26] The carrier female mice are viable and fertile, unlike males hemizygous for this mutation,[25] and they therefore provide a model in which XCI can be assessed in a range of tissues throughout development. We have shown that skewed XCI results from selection against Atrx-deficient cells at specific stages of development and differentiation in different tissues. These findings illustrate an important mechanism by which skewed XCI may occur in carriers of XLMR and provide insight into the normal role of ATRX in vivo.

Material and Methods

Atrx *Mice*

Atrx-mutant mice were generated, as described by Garrick et al.,[25] by homologous recombination in embryonic stem cells (E14, derived from 129/OlaHsd) and by injection of C57BL/6 blastocysts with the targeted cells. All wild-type mice used were F1 CBA/C57BL/6. $Atrx^{wt/null}$ females were obtained by crossing animals with a floxed *Atrx* allele and transgenic animals with Cre recombinase expressed from the *Gata1* promoter.[25,27] The $Atrx^{wt/null}$ embryos used were from crosses between these $Atrx^{wt/null}$ females and wild-type males. Mice with the floxed *Atrx* allele were also crossed with animals with a Cre recombinase transgene under the control of an inducible *Mx1* promoter (Mx1Cre).[28] Adult mice were genotyped at the *Atrx* locus by hybridizing *Sac*I-digested DNA on Southern blots with an intron 17 probe, and embryos were genotyped by PCR with primers PPS1.17 (intron 17) and PPS1.28 (exon 19) (both methods described by Garrick et al.[25]). The Mx1Cre transgene was detected by PCR (forward primer 5′-GCGGAGCCAGCACTATTTA-3′; reverse primer 5′-CCGGCATCAACGTTTTCTTTT-3′).[29]

Animal Husbandry

To obtain staged embryos, the morning on which a vaginal plug was noted was taken as embryonic day (E) 0.5. Mice were sacrificed by cervical dislocation. To obtain blood from E9.5 and E10.5 embryos, pregnant females were given an intraperitoneal heparin injection 5–10 min before they were sacrificed. Embryos were separated from the uterine wall and placenta, then were released from the yolk sac into a small volume of PBS/heparin, and were allowed to bleed out. Cre recombination was induced in mice with the floxed *Atrx* allele and Mx1Cre transgene by two intraperitoneal injections of 250 μg of the synthetic double-stranded RNA polyinosinic-polycytidylic acid (pI-pC) 2 d apart, within 3 wk after birth. Tissue analysis was performed at least 6 wk after pI-pC treatment, and the efficiency of recombination in hematopoietic samples was assessed by Southern blot after *Sac*I digestion (see above). Phenylhydrazine treatment to induce hemolytic anemia consisted of three intraperitoneal injections of 0.04 mg 1-acetyl-2-phenylhydrazine (Sigma) per g of body weight at 17.00 on day 1 and at 09.00 and 17.00 on day 2.[30] Mice were sacrificed on day 6.

Immunohistochemistry, Immunofluorescence, and FACS

Staged embryos and adult mouse tissues were fixed in 4% paraformaldehyde overnight at 4°C. After a washing in PBS, samples were dehydrated through an ethanol series and xylene and were embedded in paraffin. Before the staining, 5-μm sections were treated with Histo-Clear (Fisher Scientific) and were rehydrated. When required, antigen unmasking was performed by heat treatment in Antigen Unmasking Solution (Vector Laboratories). Sections were stained for immunohistochemistry by use of the Rabbit ABC Staining System (Santa Cruz Biotechnologies), in accordance with the manufacturer's protocol, after endogenous peroxidase activity was blocked with 3% H_2O_2. The antibodies used were rabbit polyclonal anti-ATRX H300 (Santa Cruz Biotechnologies) and normal rabbit immunoglobulin G (IgG) (Santa Cruz Biotechnologies). Cells in suspension from peripheral blood, bone marrow, fetal liver, and methylcellulose colonies were allowed to settle onto poly-L-lysine–coated coverslips, were fixed in 4% paraformaldehyde for 1 h at 4°C, and were permeabilized with 0.5% Triton-X 100 (in PBS) prior to incubation with antibodies. For fluorescence microscopy, the secondary antibodies used were Alexa 488–conjugated anti-rabbit IgG (Molecular Probes), fluorescein isothiocyanate (FITC)–conjugated anti-rabbit IgG (Jackson Laboratories), and Cy3-conjugated anti-rabbit IgG (Jackson Laboratories), and slides were mounted in Vectashield with 4′,6-diamidino-2-phenylindole (DAPI) (Vector Laboratories). To isolate erythroid cell populations by fluorescence-assisted cell sorting (FACS), single cell suspensions were incubated with a phycoerythrin (PE)–conjugated anti-TER119 antibody (BD Pharmingen) and an FITC-conjugated anti-CD71 antibody (BD Pharmingen). Gated erythroblast populations were as described by Zhang et al.[31] Briefly, early precursors were taken as CD71 medium/high, Ter199 low; intermediate precursors were CD71 high, Ter119 medium; and intermediate/late precursors were CD71 medium/high, Ter119 high.

Microscopy and Imaging

Light and fluorescence microscopy was performed using Olympus BX61 microscopes. Images were collected using OpenLab software for light microscopy and MacProbe 4.3 for fluorescence micros-

copy. Further image annotation was performed using Adobe Photoshop 7.0.

Atrx *Methylation*

DNA from 11 Atrx$^{wt/null}$ (15 samples) and 4 Atrx$^{wt/flox}$ (6 samples) adult mice was digested with *Pst*I and the methylation-sensitive enzyme *Sac*II and was analyzed by Southern blot. The probe used to detect fragments, including the *Atrx* CpG island (5′ probe), was generated by PCR (forward primer 5′-TTGCCTAACATGCACAA-AGC-3′; reverse primer 5′-ATTGGCTACGGAAATTCACC-3′). The relative intensity of bands resulting from methylated and unmethylated fragments was determined using a Typhoon PhosphoImager (Amersham Biosciences) and ImageQuant software.

Hematopoietic Progenitor Colony Culture

Hematopoietic colony-forming assays by use of E13.5 fetal liver and adult bone marrow were performed using MethoCult Media (Stem Cell Technologies 03434) in accordance with the manufacturer's guidelines. Colony type was determined by cell morphology, as described by Stem Cell Technologies. Colonies were picked after 7 d of culture or after 14 d for mixed-lineage colonies.

Results

Skewed XCI in Adult Atrx$^{wt/null}$ Mice

The targeted *Atrx* allele (*Atrx*^{flox}), described previously by Garrick et al.,[25] enables conditional knockout of the full-length isoform of Atrx by Cre-mediated recombination. Male cells hemizygous for the recombined null allele (*Atrx*^{null}) or female heterozygous cells (Atrx$^{wt/null}$) with the null allele on the active X chromosome lack expression of full-length Atrx. They can be distinguished from wild-type cells or heterozygous cells with the wild-type allele on the active X chromosome by staining with an antibody specific for full-length Atrx (H300).[25,32] Although female Atrx$^{wt/null}$ mice are viable and fertile, some do exhibit mild behavioral abnormalities, including increased aggression and hyperactivity (J.A.S., unpublished data). Preliminary data from behavioral studies showed that a proportion of heterozygotes performed poorly in a T-maze test, suggesting impaired learning and/or memory (P.M.N., unpublished data).

We initially assessed the XCI pattern in adult Atrx$^{wt/null}$ females, by immunohistochemical analysis for Atrx expression, to determine whether skewed XCI is present in mice as it is in humans. Tissues were chosen for analysis in which the majority of cells (90%–100%) expressed Atrx in wild-type samples (fig. 1). If XCI were balanced, in Atrx$^{wt/null}$ females, one would expect ~50% of the cells to lack Atrx expression due to the null allele being on the active X chromosome. In heterozygotes, the percentage of cells lacking Atrx expression was higher than in wild-type cells but remained <20% in the cerebral cortex and the granular layer of the cerebellum, as well as in the crypts of Lieberkuhn and epithelia of intestinal villi (fig. 1). Villi develop as clonal populations of cells, so each is either Atrx positive or Atrx negative. In a range of other

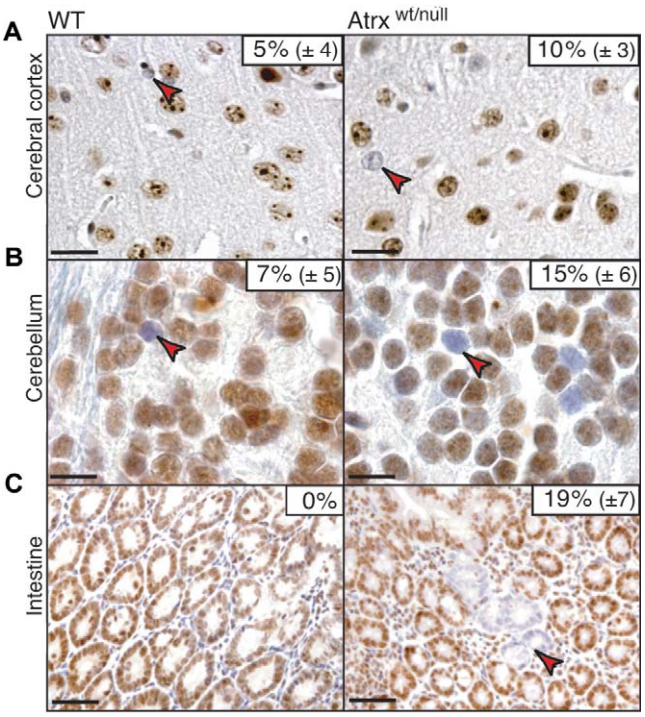

Figure 1. XCI in adult Atrx$^{wt/null}$ mice. Paraffin sections of tissues from wild-type (WT) and Atrx$^{wt/null}$ female mice, stained with the anti-Atrx antibody (H300) detected by horseradish peroxidase (*brown*) with hematoxylin counterstain (*blue*). Sections stained under the same conditions with an IgG control antibody gave a weak background signal, as shown by Garrick et al.[25] Red arrowheads indicate examples of Atrx-negative cells. The mean percentage (±1 SD) of Atrx-negative cells in the cerebral cortex and the granular layer of the cerebellum and the percentage of Atrx-negative intestinal crypts is given (three animals, with >2,000 cells or crypts per genotype). Scale bars are 25 μm (*A*), 10 μm (*B*), and 50 μm (*C*).

tissues, including kidney, ovary, and muscle, a similar bias in favor of cells expressing Atrx was observed in heterozygous samples (data not shown). The observation of <20% Atrx-negative cells in adult tissues indicates that Atrx$^{wt/null}$ mice do have skewed XCI in favor of cells with the wild-type allele on the active chromosome, similar to the situation in human female carriers of ATR-X syndrome. This analysis shows that this is a suitable model to examine the causes of skewed XCI and confirms that XCI is skewed in tissues that are inaccessible in humans.

No Effect of Atrx Mutation on Primary Pattern of XCI or Early Cell Selection

To determine whether skewed XCI in ATR-X carrier females is likely to be because of an effect of *ATRX* mutation on the primary pattern of XCI or secondary selection events during development, we assessed the XCI pattern in E8 embryos. At E8, Atrx$^{wt/null}$ embryos are mosaics of

Atrx-expressing and -nonexpressing cells (fig. 2*A*), with Atrx-negative cells present in all three primary germ layers (endoderm, ectoderm, and mesoderm) at ~40% of the total cell number.

Because Atrx-negative cells were found throughout the embryo, it seems that there is no strong selection against these cells during the establishment of XCI or in the designation of the germ layers. The reduced percentage of negative cells (~40%) could be explained either by a weak competitive disadvantage of the null cells or by a bias in the original XCI ratio due to heterozygosity at the *Xce* locus, which can cause a bias in the choice of XCI.[3–6] However, the skewed XCI observed in adults must result from secondary selection events that occur later in embryonic development.

Skewed XCI Due to Cell Selection during Tissue Formation

We performed a systematic, detailed analysis of the XCI pattern in a range of tissues at different stages of development. Atrx can be detected in virtually all cells of wild-type embryos throughout gestation (fig. 3), but skewed XCI (ratio >80:20) was apparent in most tissues by late gestation (E17.5) in Atrx$^{wt/null}$ mice (fig. 2*B*). However, although the overall impression for the embryo as a whole is of a gradual decline in Atrx-null cells during development, at the level of individual tissues, the degree of cell selection varied significantly. For example, at E14.5 (fig. 2*B* and 2*C*), the percentage of negative cells remained 30%–40% in the forebrain and dermis (mesenchyme) but had declined to <20% in the epidermis and dorsal root

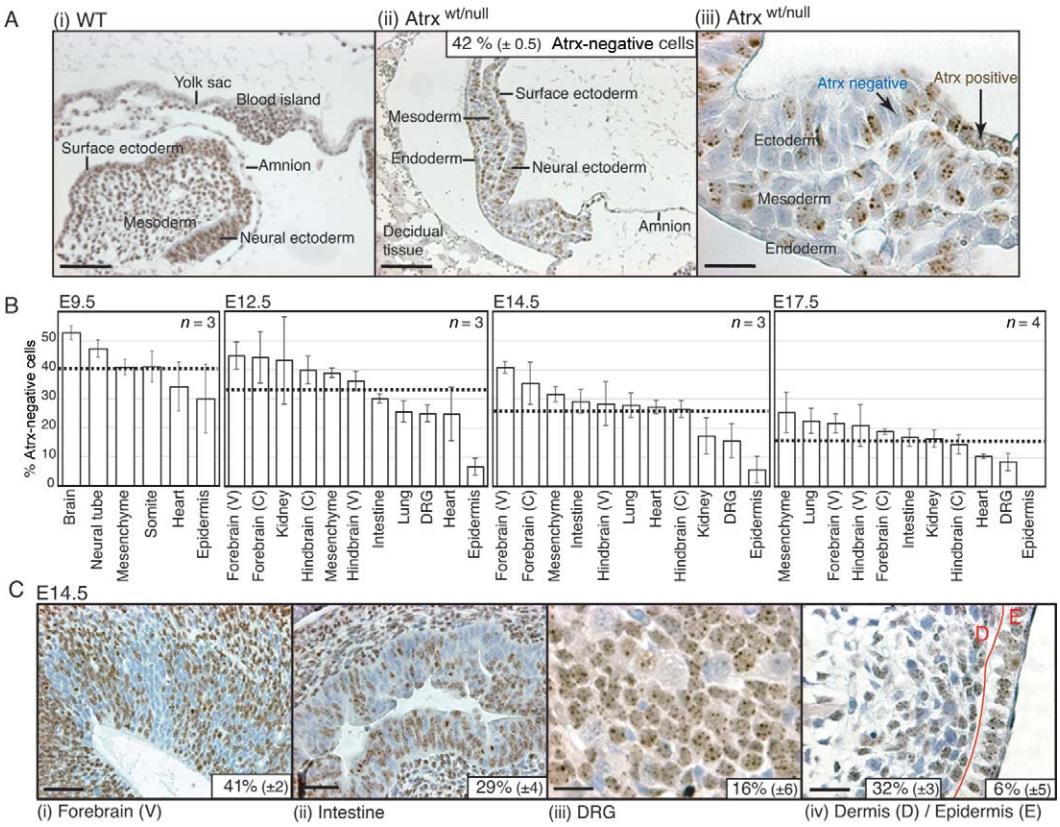

Figure 2. Pattern of XCI during embryonic development. *A,* Paraffin sections of ~E8 wild-type (WT) and Atrx$^{wt/null}$ littermate embryos, stained with the anti-Atrx antibody (H300) and hematoxylin counterstain (as in fig. 1). Examples of Atrx-positive and -negative cells are indicated in panel iii. The mean percentage Atrx-negative cells (±1 SD) was calculated from three Atrx$^{wt/null}$ embryos (>2,000 cells were scored in total). The punctate nuclear staining observed at higher magnification (*iii*) is typical for Atrx localization at heterochromatic foci. Scale bars are 100 μm (*i* and *ii*) and 25 μm (*iii*). *B,* Percentage of cells negative for Atrx at E9.5, E12.5, E14.5, and E17.5, scored by staining the tissue sections as in panel A. Each bar is the mean of percentages from a number of embryos (*n*); error bars are ±1 SD. The number of cells scored per tissue per embryo is 100–1,000 at E9.5 and 500–2,500 at other stages. The horizontal dashed line indicates the mean of the values from all the tissues shown at each time point and is an estimate of the overall percentage of Atrx-negative cells. C = the postmitotic zone of the developing brain cortex; DRG = dorsal root ganglia; V = proliferative ventricular zone. *C,* Examples of Atrx$^{wt/null}$ tissues at E14.5, stained as in panel A, with the percentage of Atrx-negative cells shown. Scale bars are 50 μm (*i* and *ii*) and 25 μm (*iii* and *iv*).

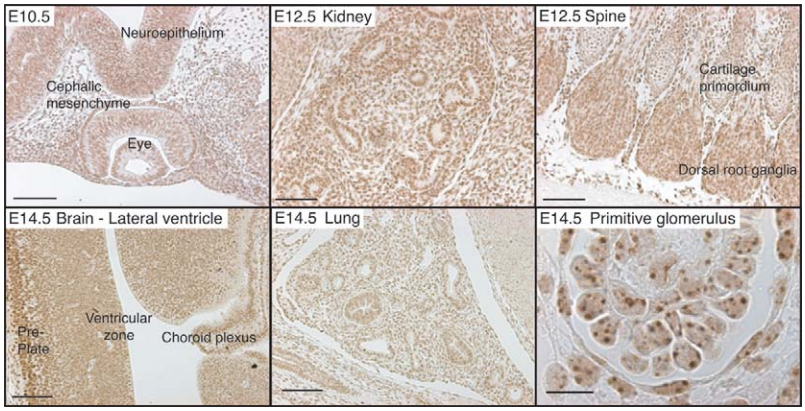

Figure 3. Widespread expression of Atrx during embryonic development. Representative paraffin sections of wild-type mouse embryos at the stages indicated were stained with an anti-Atrx antibody (H300, with HRP detection). At higher magnification (of E14.5 primitive glomerulus), punctate nuclear localization at heterochromatic loci is observed. The level of Atrx protein is not uniform in all tissues—for example, there is stronger staining in the postmitotic preplate than in the proliferative ventricular zone of the developing brain. Scale bars are 10 μm for the primitive glomerulus and 100 μm for all other images.

ganglia. These data indicate that skewed XCI is a result of secondary cell selection but, interestingly, suggest that the selection pressure varies between cell lineages.

Stability of XCI Status

We next considered the possibility of whether the high proportion of Atrx-positive cells could alternatively be explained by reactivation of the silent wild-type allele. Many gene promoters on the inactive X chromosome are characterized by methylated CpG islands, whereas these loci are unmethylated on the active X. Therefore, females normally have an ~50:50 ratio of methylated:unmethylated X-chromosome CpG island alleles. Reactivation of the silent allele would be expected to result in loss of methylation of that allele, detectable by a deviation from the ~50:50 methylation ratio. We assessed the ratio of methylated:unmethylated *Atrx* alleles in $Atrx^{wt/null}$ mice and females without Cre recombination ($Atrx^{wt/flox}$), using a methylation-sensitive restriction digest (fig. 4), and found an ~50:50 ratio overall in both genotypes. Although CpG island methylation is an indirect assay for gene silencing, this suggested that the XCI status of $Atrx^{wt/null}$ cells is stable. This conclusion is also supported by the observation that, within the clonal cell populations of intestinal villi, all cells are either Atrx negative or Atrx positive (fig. 1), which would be unlikely if spontaneous reactivation of the silent allele occurred. Therefore, we can be confident that cell selection is the mechanism that results in the increase in the proportion of Atrx-expressing cells.

XCI in Hematopoiesis

Having determined that cell selection underlies skewed XCI in carriers of an *Atrx* mutation, we next addressed the question of whether selection is continual (i.e., due to a general cellular defect affecting viability or proliferation, as has been proposed for XLMR mutations) or limited to particular stages of differentiation or development.

We initially analyzed skewing in the hematopoietic system, because blood lineages are highly skewed in carriers of ATR-X syndrome mutations.[23] Embryonic hematopoiesis is divided into two phases, both of which were analyzed: the transient production of erythroblasts in the yolk sac ("primitive" erythropoiesis), followed by the emergence of hematopoietic stem cells (HSCs) and establishment of "definitive" erythropoiesis in the fetal liver and subsequently the bone marrow.

Primitive erythrocytes emerge from yolk sac mesoderm at E7.5–E9 and continue to divide and differentiate in a semisynchronous manner in circulation after release from the blood islands.[33–35] The pattern of XCI at three sequential stages of primitive erythroblast maturation was determined by scoring the proportion of Atrx-negative erythroid cells in yolk sac blood islands at E8 and in circulation at E9.5 and E10.5 (fig. 5). The percentage of negative cells remained constant at ~30% over this time period, indicating that there is no continuing selection as primitive erythroblasts undergo maturation and proliferation. However, the percentage of Atrx-negative erythroblasts (~30%) was lower than the percentage in the embryo overall at E8 (~40%), suggesting that a lack of Atrx may slightly reduce the probability of a cell participating in blood island formation.

Differentiation of definitive erythroid cells from HSCs can be broadly divided into the specification of the erythroid program in multipotent progenitor cells, followed by the differentiation and maturation of committed erythroid precursors (fig. 6*A*).[36] This process is established in the fetal liver in midgestation mouse embryos and continues in the bone marrow throughout adult life. We isolated cells at early, intermediate, and late stages of mat-

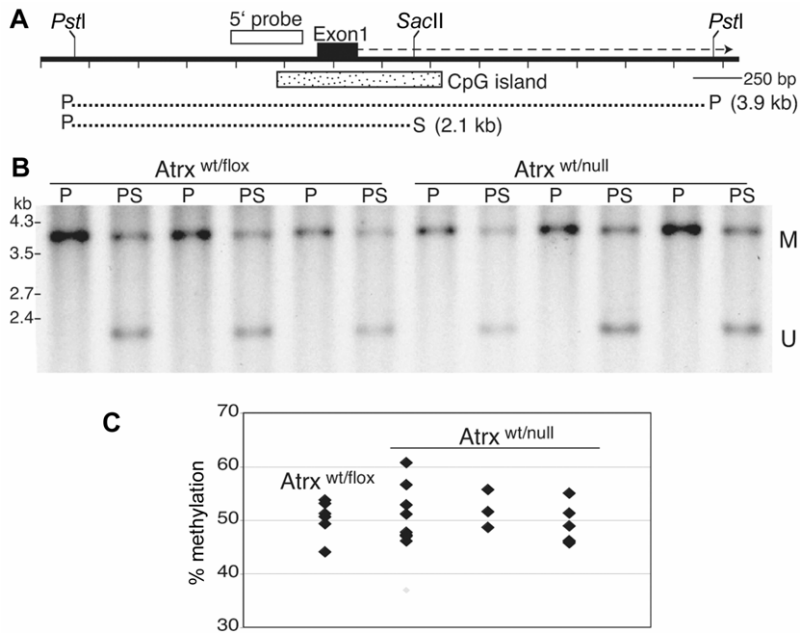

Figure 4. Methylation of the *Atrx* promoter. *A,* Schematic representation of the 5′ end of *Atrx,* showing the position of the CpG island and direction of transcription. The size of fragments generated by digesting genomic DNA with the restriction enzyme *Pst*I alone (P) or with both *Pst*I and the methylation-sensitive enzyme *Sac*II (S) is indicated. *B,* Southern-blot analysis (with use of the 5′ probe shown in panel A) of DNA from adult female Atrx$^{wt/flox}$ and Atrx$^{wt/null}$ mice after digestion with the two enzymes. M = fragment obtained from alleles with a methylated CpG island; U = fragment obtained from unmethylated copies of this sequence that are cut by both *Pst*I and *Sac*II. *C,* Ratio of M:U calculated for each sample (shown as percentage of the total signal). Each group of points is from a separate Southern blot and includes a range of tissue types (including brain, intestine, tail, ovary, and kidney). The example shown in panel B is from tail DNA samples.

uration from E14.5 Atrx$^{wt/null}$ fetal livers by FACS. Almost identically high proportions of Atrx-positive cells were observed at all stages of maturation in both genotypes (fig. 6*B*). The lack of Atrx-negative cells in Atrx$^{wt/null}$ samples showed that XCI was almost completely skewed, indicating strong selection against cells lacking Atrx at an earlier stage in erythropoiesis.

To study cells from earlier stages in differentiation, hematopoietic progenitor colonies were grown in methylcellulose medium from Atrx$^{wt/null}$ and wild-type E13.5 fetal liver and adult bone marrow, and Atrx expression in the clonogenic colonies was assayed by immunofluorescence. Virtually no Atrx-negative colonies were found, irrespective of whether the colonies were from committed erythroid, myeloid, or multilineage progenitors (fig. 6*C*). Therefore, the XCI ratio is highly skewed at both the progenitor and precursor stages of definitive erythropoiesis, so cell selection must occur during the very earliest steps in development of the hematopoietic system. These observations suggest that skewed XCI in adult blood lineages is likely to be because of events during embryogenesis, rather than selection during continual renewal of blood cells.

Therefore, we were interested to determine when selection occurred during formation of HSCs. A major site of emergence of definitive HSCs is the ventral wall of the dorsal aorta in the aorta-gonads-mesonephros region of the embryo at ~E10.5. Intra-aortic clusters of cells have been demonstrated to contain cells with HSC activity[37–39] and can be observed by sectioning the embryos at this stage of development. All cells in intra-aortic clusters express Atrx in wild-type embryos (data not shown), but, although both positive and negative cells were observed in Atrx$^{wt/null}$ embryos (fig. 6*D*), the percentage of Atrx-negative cells in the clusters was only ~15% (fig. 6*E*). This suggests a stronger selective pressure at the earliest stage of definitive hematopoiesis, compared with primitive hematopoiesis (~30% Atrx-negative cells). The observation of cell selection in intra-aortic clusters, in conjunction with the almost complete absence of Atrx-negative cells at all stages of definitive erythropoiesis, strongly suggest that selection during the establishment of the stem cell population in the embryo results in highly skewed XCI in adult blood.

Restricted Rather Than Continuous Cell Selection

To address whether selection is restricted or continuous in definitive erythropoiesis, we circumvented selection against Atrx-deficient cells during embryonic development by using an inducible Cre recombinase in postnatal mice. Recombination between Lox P sites can be induced

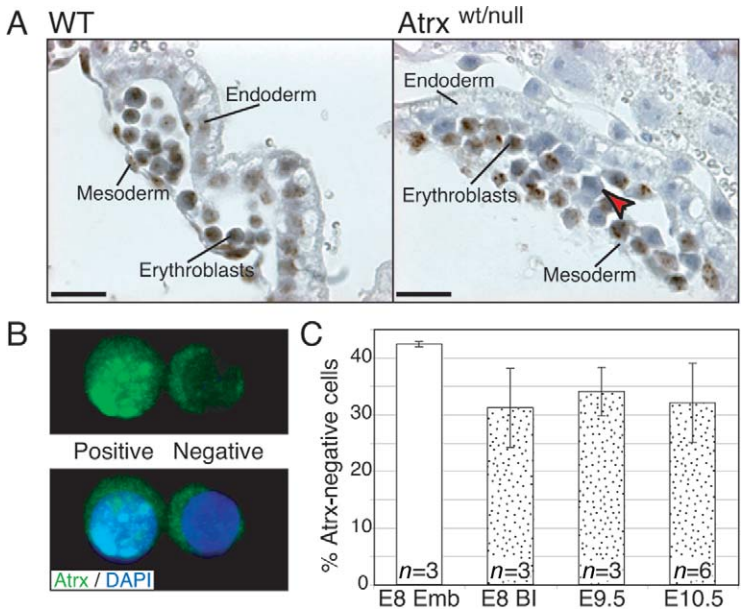

Figure 5. XCI in primitive erythropoiesis. Primitive erythroblasts in yolk sac blood islands at E8 (*A*) and in circulation at E9.5 and E10.5 (*B*). *A,* Paraffin sections through the yolk sac of littermate wild-type (WT) and Atrx$^{wt/null}$ E8 embryos stained with an anti-Atrx antibody (with hematoxylin counterstain). The red arrowhead indicates an example of an Atrx-negative erythroblast. Scale bars are 25 μm. *B,* Representative example of a pair of erythroid cells from Atrx$^{wt/null}$ E9.5 blood, stained for Atrx (*green*) and DAPI (*blue*). One nucleus is Atrx positive, and the other is Atrx negative. All wild-type cells were Atrx positive. Both cells show some cytoplasmic background. *C,* Percentage of Atrx-negative cells within embryonic tissues at E8 (E8 Emb) (see also fig. 2) and primitive erythroblasts in blood islands at E8 (E8 BI) and in circulation at E9.5 and E10.5. Approximately 750 cells in blood islands were scored from three embryos, and ~500 peripheral blood cells were scored at E9.5 (three embryos) and E10.5 (six embryos). Error bars are ± 1 SD.

in mice with a Cre recombinase transgene under the control of the inducible *Mx1* promoter, by injection with interferon or the double-stranded RNA pI-pC.[28] We crossed mice with the floxed *Atrx* allele to Mx1Cre transgenic mice and injected female Atrx$^{wt/flox}$ and male Atrx^{flox} pups with pI-pC. Recombination using this method is not ubiquitous but has been reported to be efficient in the hematopoietic system,[28,40] and we confirmed this by Southern-blot analysis of bone marrow and spleen samples (fig. 7*A*). At least 6 wk after pI-pC treatment, the percentage of Atrx-negative cells in the bone marrow of female heterozygous mice was ~20%–35% (fig. 8*A*).

Although there is continual turnover of hematopoietic cells, we determined whether increased proliferation would result in increased cell selection by inducing stress erythropoiesis by phenylhydrazine treatment. Because phenylhydrazine causes hemolytic anemia, it triggers rapid proliferation of erythroid cells in the bone marrow and spleen.[30] However, this pressure on erythropoiesis did not alter the proportion of Atrx-negative cells in heterozygous female mice (fig. 8*B*). Therefore, XCI does not become severely skewed in adult erythropoiesis, irrespective of the rate of cell division. In addition, a hematopoietic progenitor colony assay with the use of bone marrow from a pI-pC treated female Atrx$^{wt/flox}$ Mx1Cre mouse resulted in an ~50:50 ratio of positive:negative colonies, indicative of balanced XCI (fig. 8*B*). Also, male Atrx^{flox}/Y Mx1Cre mice, in which recombination to Atrx^{null} was induced postnatally, were also viable and apparently able to produce normal blood in the absence of Atrx (figs. 7*B* and 8*A*), suggesting that Atrx is not essential for adult erythropoiesis.

These results from whole bone marrow and bone marrow progenitor colonies after postnatal ablation of Atrx, showing a significant proportion of Atrx-negative cells, contrast dramatically with the almost complete lack of Atrx-negative cells at all stages of definitive erythropoiesis in mice with an inherited *Atrx* mutation and to the highly skewed XCI in female carriers of ATR-X syndrome. This suggests that, although Atrx is important during embryonic development of the hematopoietic system, there is no major requirement for Atrx during adult hematopoiesis in the bone marrow. This means that, in the specific case of hematopoiesis, cell selection is not a continuous process.

To test the generality of this conclusion, we compared the proportion of Atrx-negative cells in tissue sections from pI-pC–treated Atrx^{flox}/Y Mx1Cre males (to assess the efficiency of Mx1Cre-mediated recombination), pI-pC–treated Atrx$^{wt/flox}$ Mx1Cre females, and Atrx$^{wt/null}$ females with an inherited null allele (fig. 8*C*). In both the crypts/villi of the intestine and the glomerular cells of the kidney,

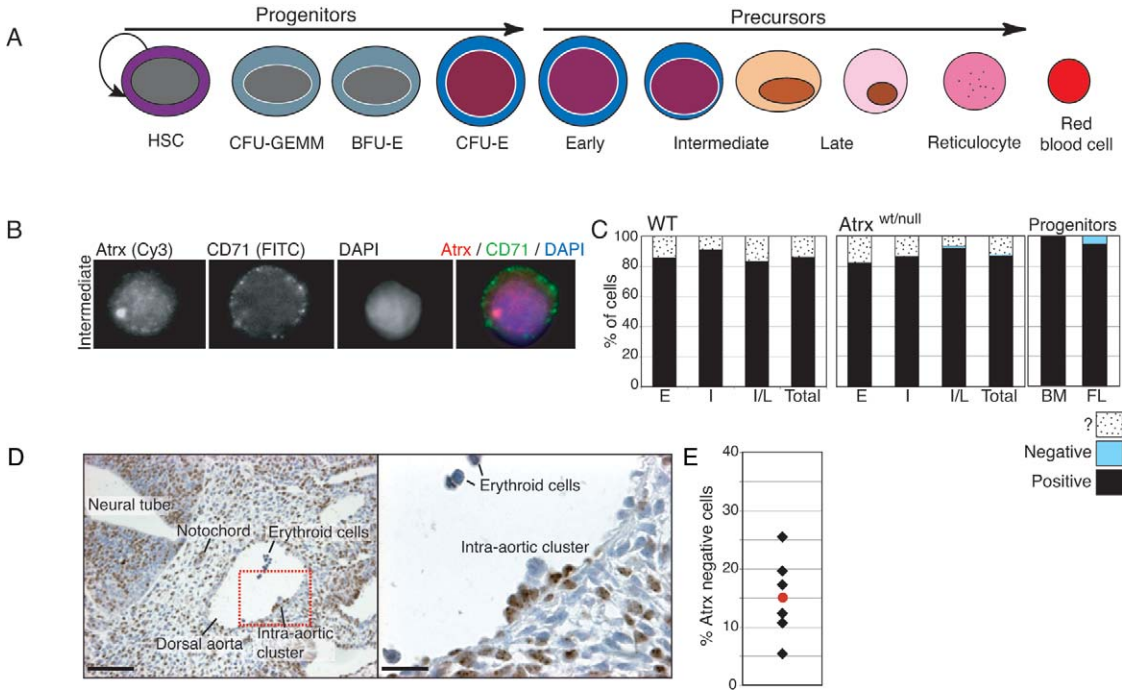

Figure 6. Highly skewed XCI in definitive erythropoiesis. *A,* Schematic representation of the definitive erythropoietic lineage. Differentiation of HSCs proceeds through a series of progenitor and precursor cells. CFU-GEMM = colony-forming unit–granulocyte/erythroid/macrophage/megakaryocyte; BFU-E = burst forming unit–erythroid; CFU-E = colony-forming unit–erythroid. *B* and *C,* Cells at early (E), intermediate (I), and late (L) stages of erythroid differentiation (see panel A) were isolated by FACS (sorted with antibodies against CD71 and Ter119) from E14.5 wild-type and Atrx$^{wt/null}$ fetal livers. *B,* Example of intermediate stage cells stained with H300 antibody and DAPI. The FITC-conjugated CD71 antibody used in FACS is also visible by immunofluorescence. Atrx is typically observed at concentrated nuclear foci in intermediate and late cells and in a punctate nuclear pattern in early erythroid cells. In panel C, cells in each population were scored as Atrx negative, Atrx positive, or ambiguous/unclear staining (denoted by ?), shown as a percentage of the total number of cells analyzed. Scores are pooled from two wild-type (WT) and two Atrx$^{wt/null}$ embryos (total of ~350 Atrx$^{wt/null}$ cells). Bone marrow (BM) from an Atrx$^{wt/null}$ adult and fetal liver (FL) from three E13.5 Atrx$^{wt/null}$ embryos were cultured in methylcellulose-based medium to obtain hematopoietic progenitor colonies, which were then stained and scored for Atrx expression. Colony type was determined by cell morphology and included granulocyte/macrophage colonies, erythroid and erythroid/megakaryocyte colonies, macrophage colonies, and mixed colonies containing cells from multiple lineages. The few Atrx-negative colonies were not restricted to a particular lineage. *D* and *E,* Intra-aortic clusters in Atrx$^{wt/null}$ embryos. *D,* Representative example of a paraffin section from an E10.5 Atrx$^{wt/null}$ embryo, cut in transverse orientation through the trunk, stained for Atrx. All cells in comparable sections from wild-type embryos were Atrx positive. An intra-aortic cluster and other features are marked, with the boxed area shown at higher magnification on the right. Scale bars are 100 μm (*left*) and 25 μm (*right*). *E,* Percentage of Atrx-negative cells within intra-aortic clusters in six embryos (*black diamonds*) and the mean (*red dot*), for a total of ~500 cells scored.

a much higher proportion of Atrx-negative cells remained in the mice with postnatal ablation of Atrx than in those bearing the null allele, throughout embryogenesis. This suggested that, in general, cell selection resulting in skewed XCI is restricted to particular stages of development in carriers of an *Atrx* mutation.

Discussion

Skewed XCI Caused by Cell Selection, Not a General Cellular Defect

It is widely assumed that, in the majority of monogenic X-linked disorders associated with skewed XCI, the skewing is a result of cells with the mutant allele on the active chromosome being outcompeted by cells expressing the normal allele. We have shown, using a mouse model, that mutation of the XLMR gene *Atrx* does indeed lead to skewed inactivation due to cell selection during embryogenesis. The initial XCI pattern is balanced, indicating that loss of Atrx does not cause skewing by altering the choice of which chromosome is inactivated. Therefore, we have demonstrated that the assumption of cell selection is likely to be valid for cases such as ATR-X syndrome.

Carriers of ATR-X syndrome mutations have skewed XCI in multiple tissues,[23] and it has been proposed that many XLMR mutations may lead to widespread skewing due to a general defect in cell viability or proliferation.[12] However, the evidence presented here strongly suggests that

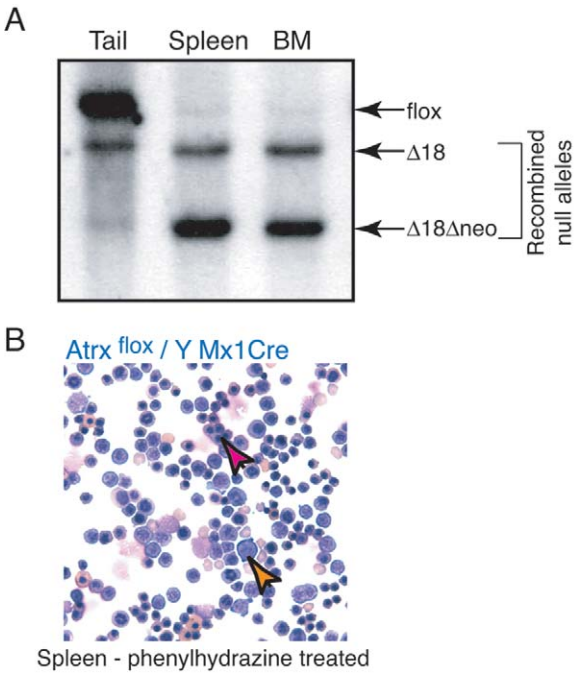

Figure 7. Mx1Cre-mediated recombination in hematopoietic tissues. *A,* Example of an *Sac*I-digest Southern blot with DNA from an Atrx^{flox}/Y Mx1Cre male mouse after pI-pC–induced recombination and phenylhydrazine treatment, showing samples taken from the tail, spleen, and bone marrow (BM). The intron 17 probe distinguishes the *Atrx^{flox}* (flox) and the recombined null alleles (Δ18 and Δ18Δneo), as described by Garrick et al.[25] Recombination is highly efficient in the spleen and bone marrow but not in the tail. *B,* Cytospin (stained with modified Wright's stain) of spleen cells from a phenylhydrazine-treated recombined Atrx^{flox}/Y Mx1Cre male mouse. An example of a polychromatic/orthochromatic erythroblast is indicated by a red arrow, and a proerythroblast by an orange arrow, demonstrating that erythropoiesis can occur in the absence of Atrx.

the defect caused by loss of Atrx only causes a selective disadvantage at discrete stages of development. One would predict that a general cellular defect would result in early and/or continuous selection, and yet we have found that processes involving multiple cell divisions, such as stress-induced adult hematopoiesis, can occur with no major selection. We suggest, therefore, that it should not be assumed that the presence of skewed XCI throughout the body is caused by either an event early in embryogenesis or a general cellular defect. This may be the case for some X-linked mutations, but loss of Atrx causes multiple, apparently independent selection events at different times in different tissues.

The ATRX Mouse Model

By necessity, this work has relied on a mouse model to be able to analyze a wide range of tissues throughout embryogenesis. Therefore, certain caveats must be considered when this data is used to understand the human disorder. The *Atrx* mutation studied is a null allele, in contrast with ATR-X syndrome mutations that, to date, all appear to be hypomorphic (R.J.G., unpublished data). This difference may account for the more marked phenotype of Atrx$^{wt/null}$ mice compared with female carriers of ATR-X syndrome. In addition, it is also possible that the groups of genes affected by ATRX are not identical in human and mouse. Therefore, the details of time and location of ATRX requirement, and thus the skewing of XCI, may differ between species. However, given the high level of conservation in the protein sequence, localization, and interaction partners,[17,26,41,42] it seems reasonable to assume that the principles described here apply to ATR-X syndrome.

Role of ATRX in Development

In addition to providing an example of how an X-linked mutation leads to skewed XCI, this study also gives some insight into the role of ATRX in development, which may be important for understanding ATR-X syndrome. It was initially surprising that selection against cells lacking Atrx did not occur early in embryogenesis in most tissues, that a notable number of these cells persisted in adult animals, and that postnatal ablation of Atrx in males resulted in apparently normal blood in the complete absence of this protein. However, these data, which indicate that Atrx is not necessary for basic cell viability or division, are consistent with previous studies. Although Atrx-null male embryos die by E9.5 during gestation, they are able to complete gastrulation and are generally morphologically normal.[25] The lethal phenotype appears to be due to a specific defect in trophoblast development. Similarly, neuronal progenitors lacking Atrx exhibit increased apoptosis only after 6 d of differentiation, not in the undifferentiated state.[32] Surviving null neurons express normal markers, such as MAP2 and NF200. Collectively, this evidence suggests that ATRX is most important when a cell negotiates specific stages of differentiation or development. Mechanistically, this could be explained by the stages at which target genes regulated by ATRX are required. Since ATR-X syndrome has a distinct set of phenotypic features, these could thus result from defects at specific stages of tissue formation, rather than from the same problem in multiple cell types.

XCI and Understanding of X-Linked Disorders

In this mouse model, we do not see a clear correlation between tissues that have severely skewed XCI and tissues affected in ATR-X syndrome. Indeed, a general question remains as to why, in a number of XLMR disorders, skewed XCI occurs in female carriers in tissues where there is no apparent phenotype in affected males (such as in buccal cells and hair roots of ATRX-mutation carriers).[12,23] A possible explanation is the sensitivity of the competitive situation present in heterozygous females, in which even a

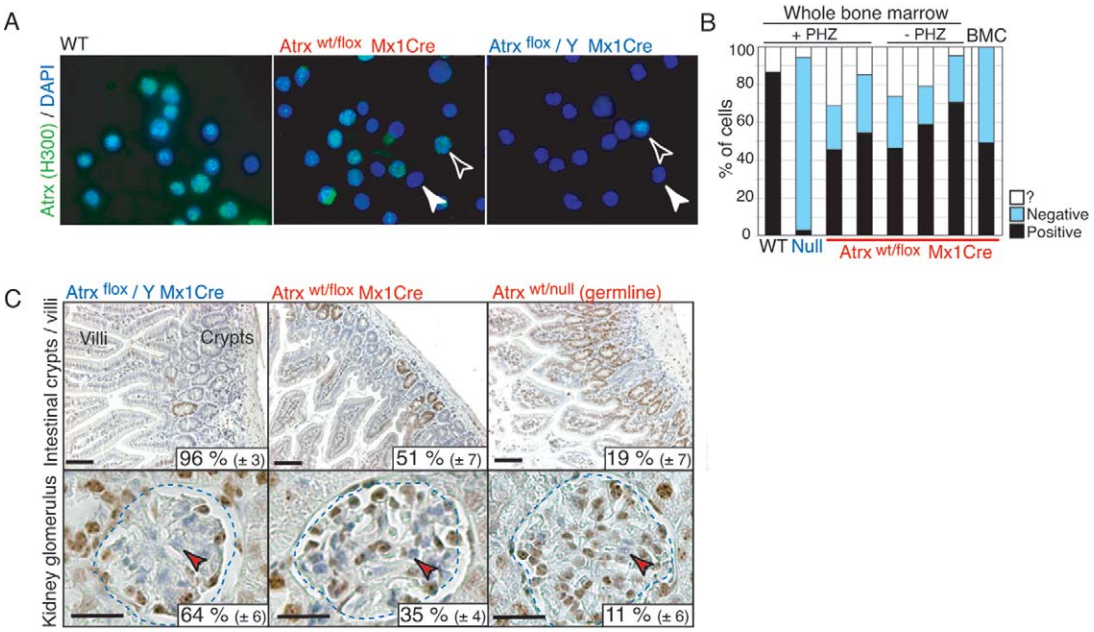

Figure 8. Restricted, not continuous, cell selection. *A* and *B,* Atrx ablated postnatally in mice with a floxed *Atrx* allele by induction of a Cre recombinase transgene controlled by the *Mx1* promoter (Mx1Cre). Atrx expression was examined by immunofluorescence in bone marrow cells from wild-type (WT) adult mice, $Atrx^{wt/flox}$ Mx1Cre females, and an $Atrx^{flox}$/Y Mx1Cre male. *A,* Bone marrow, after phenylhydrazine treatment to induce stress erythropoiesis, stained for Atrx expression (with H300 as the primary antibody and Alexa 488-conjugated as the secondary antibody) and with DAPI. Filled arrowheads indicate examples of Atrx-negative cells, and open arrowheads indicate examples of Atrx-positive cells. *B,* Percentage of Atrx-negative, Atrx-positive, or ambiguous (denoted by ?) cells in bone marrow samples, scored by staining as in panel A. Each bar represents an individual animal (~150 cells scored per mouse), with phenylhydrazine treatment (+PHZ) or without it (−PHZ). "Null" represents a recombined $Atrx^{flox}$/Y Mx1Cre male. "BMC" shows the percentage of Atrx-positive and -negative hematopoietic progenitor colonies obtained by methylcellulose culture of $Atrx^{wt/null}$ Mx1Cre bone marrow (total of 89 bone marrow colonies). *C,* Paraffin sections of intestine and kidney from adult mice with the genotypes shown, stained with the anti-Atrx antibody H300 as above. In wild-type mice, all intestinal villi and glomerular cells are positive for Atrx expression (see also fig. 1). "Germline" refers to mice inheriting the null *Atrx* allele through the maternal germline. Three $Atrx^{flox}$/Y Mx1Cre, four $Atrx^{wt/flox}$ Mx1Cre, and four $Atrx^{wt/null}$ (germline) mice were analyzed. The percentage of Atrx-negative crypts/villi (>500 crypts per genotype) and the percentage of Atrx-negative kidney glomerular cells (>300 glomerular cells within dashed line [*arrows*]) were scored; the mean percentage (±1 SD) is shown. The percentage of negative cells in $Atrx^{flox}$ Mx1Cre males gives an indication of the efficiency of recombination after pI-pC treatment (i.e., 100% negative cells would indicate 100% recombination). Scale bars are 100 μm for intestine and 20 μm for kidney.

slight disparity between maternally and paternally expressing cells is likely to result in the dominance of one population. By contrast, in males, a subtle defect may not result in an observable phenotype. If not all cells are affected equally, there may be competition in the male between more or less severely affected cells. A similar phenomenon has been described in comparisons of the sensitivity of detection of defects in chimeric mice and in complete knockout mice. In chimeric animals, analogous to heterozygous females, cell selection can be observed in tissues that showed no apparent phenotype in complete knockout mice, enabling the identification of new sites of action of genes.[43–46] In addition, in the case of Atrx, the continued survival of some null cells suggests that, once past particular steps in development, cells lacking Atrx are no longer at a disadvantage and appear phenotypically normal. Therefore, in males, it may be that, if sufficient cells can overcome these developmental "hurdles," the tissue can develop relatively normally.

Overall, this study has demonstrated how skewed XCI can be established over the course of development by tissue-specific cell selection. This work suggests that the assumption that mutations in XLMR genes such as *ATRX* confer a selective disadvantage is valid but indicates that widespread skewing is not necessarily a result of a general defect in cell viability or proliferation. In terms of furthering our understanding of X-linked disorders, alteration of the XCI pattern is a sensitive indicator of gene function. In the case of ATR-X syndrome, this study of XCI points toward ATRX as having importance at particular stages of tissue differentiation, and this will direct future experiments to identify target genes regulated by ATRX that may be responsible for this pattern. It is possible that establishment of how skewed XCI emerges may be a

useful tool for gaining insight into the roles of other genes responsible for developmental disorders.

Acknowledgments

We thank Ann Atzberger and Craig Waugh, for technical assistance with cell sorting, and Marella de Bruijn and Francisco Iborra, for advice.

Web Resources

The accession number and URLs for data presented herein are as follows:

GenBank, http://www.ncbi.nlm.nih.gov/Genbank/ (for Atrx [accession number NM_009539])
Online Mendelian Inheritance in Man (OMIM), http://www.ncbi.nlm.nih.gov/Omim/ (for ATR-X syndrome)

References

1. Lyon MF (1961) Gene action in the X-chromosome of the mouse (*Mus musculus L*). Nature 190:372–373
2. Amos-Landgraf JM, Cottle A, Plenge RM, Friez M, Schwartz CE, Longshore J, Willard HF (2006) X chromosome-inactivation patterns of 1,005 phenotypically unaffected females. Am J Hum Genet 79:493–499
3. Cattanach BM, Isaacson JH (1967) Controlling elements in the mouse X chromosome. Genetics 57:331–346
4. Chadwick LH, Pertz LM, Broman KW, Bartolomei MS, Willard HF (2006) Genetic control of X chromosome inactivation in mice: definition of the *Xce* candidate interval. Genetics 173: 2103–2110
5. Chadwick LH, Willard HF (2005) Genetic and parent-of-origin influences on X chromosome choice in *Xce* heterozygous mice. Mamm Genome 16:691–699
6. Courtier B, Heard E, Avner P (1995) *Xce* haplotypes show modified methylation in a region of the active X chromosome lying 3′ to *Xist*. Proc Natl Acad Sci USA 92:3531–3535
7. Belmont JW (1996) Genetic control of X inactivation and processes leading to X-inactivation skewing. Am J Hum Genet 58:1101–1108
8. Brown CJ, Robinson WP (2000) The causes and consequences of random and non-random X chromosome inactivation in humans. Clin Genet 58:353–363
9. Puck JM, Willard HF (1998) X inactivation in females with X-linked disease. N Engl J Med 338:325–328
10. Hendriks RW, Kraakman ME, Schuurman RK (1992) X chromosome inactivation patterns in haematopoietic cells of female carriers of X-linked severe combined immunodeficiency determined by methylation analysis at the hypervariable DXS255 locus. Clin Genet 42:114–121
11. Allen RC, Nachtman RG, Rosenblatt HM, Belmont JW (1994) Application of carrier testing to genetic counseling for X-linked agammaglobulinemia. Am J Hum Genet 54:25–35
12. Plenge RM, Stevenson RA, Lubs HA, Schwartz CE, Willard HF (2002) Skewed X-chromosome inactivation is a common feature of X-linked mental retardation disorders. Am J Hum Genet 71:168–173
13. Gibbons RJ, Brueton L, Buckle VJ, Burn J, Clayton-Smith J, Davison BC, Gardner RJ, Homfray T, Kearney L, Kingston HM, et al (1995) Clinical and hematologic aspects of the X-linked alpha-thalassemia/mental retardation syndrome (ATR-X). Am J Med Genet 55:288–299
14. Gibbons RJ, Higgs DR (2000) Molecular-clinical spectrum of the ATR-X syndrome. Am J Med Genet 97:204–212
15. Gibbons RJ, Wada T (2004) ATRX mutations and X-linked alpha thalassaemia mental retardation syndrome. In: Epstein CJ, Erickson RP, Wynshaw-Boris A (eds) Inborn errors of development. Oxford University Press, Oxford
16. Weatherall DJ, Higgs DR, Bunch C, Old JM, Hunt DM, Pressley L, Clegg JB, Bethlenfalvay NC, Sjolin S, Koler RD, et al (1981) Hemoglobin H disease and mental retardation: a new syndrome or a remarkable coincidence? N Engl J Med 305:607–612
17. Xue Y, Gibbons R, Yan Z, Yang D, McDowell TL, Sechi S, Qin J, Zhou S, Higgs D, Wang W (2003) The ATRX syndrome protein forms a chromatin-remodeling complex with Daxx and localizes in promyelocytic leukemia nuclear bodies. Proc Natl Acad Sci USA 100:10635–10640
18. Gibbons RJ, McDowell TL, Raman S, O'Rourke DM, Garrick D, Ayyub H, Higgs DR (2000) Mutations in ATRX, encoding a SWI/SNF-like protein, cause diverse changes in the pattern of DNA methylation. Nat Genet 24:368–371
19. Picketts DJ, Higgs DR, Bachoo S, Blake DJ, Quarrell OW, Gibbons RJ (1996) ATRX encodes a novel member of the SNF2 family of proteins: mutations point to a common mechanism underlying the ATR-X syndrome. Hum Mol Genet 5:1899–1907
20. Gecz J, Pollard H, Consalez G, Villard L, Stayton C, Millasseau P, Khrestchatisky M, Fontes M (1994) Cloning and expression of the murine homologue of a putative human X-linked nuclear protein gene closely linked to PGK1 in Xq13.3. Hum Mol Genet 3:39–44
21. Gibbons RJ, Picketts DJ, Villard L, Higgs DR (1995) Mutations in a putative global transcriptional regulator cause X-linked mental retardation with alpha-thalassemia (ATR-X syndrome). Cell 80:837–845
22. Stayton CL, Dabovic B, Gulisano M, Gecz J, Broccoli V, Giovanazzi S, Bossolasco M, Monaco L, Rastan S, Boncinelli E, et al (1994) Cloning and characterization of a new human Xq13 gene, encoding a putative helicase. Hum Mol Genet 3: 1957–1964
23. Gibbons RJ, Suthers GK, Wilkie AO, Buckle VJ, Higgs DR (1992) X-linked alpha-thalassemia/mental retardation (ATR-X) syndrome: localization to Xq12-q21.31 by X inactivation and linkage analysis. Am J Hum Genet 51:1136–1149
24. Chelly J, Mandel JL (2001) Monogenic causes of X-linked mental retardation. Nat Rev Genet 2:669–680
25. Garrick D, Sharpe JA, Arkell R, Dobbie L, Smith AJ, Wood WG, Higgs DR, Gibbons RJ (2006) Loss of Atrx affects trophoblast development and the pattern of X-inactivation in extraembryonic tissues. PLoS Genet 2:e58
26. Picketts DJ, Tastan AO, Higgs DR, Gibbons RJ (1998) Comparison of the human and murine ATRX gene identifies highly conserved, functionally important domains. Mamm Genome 9:400–403
27. Mao X, Fujiwara Y, Orkin SH (1999) Improved reporter strain for monitoring Cre recombinase-mediated DNA excisions in mice. Proc Natl Acad Sci USA 96:5037–5042
28. Kuhn R, Schwenk F, Aguet M, Rajewsky K (1995) Inducible gene targeting in mice. Science 269:1427–1429
29. Roebroek AJ, Taylor NA, Louagie E, Pauli I, Smeijers L, Snellinx A, Lauwers A, Van de Ven WJ, Hartmann D, Creemers

JW (2004) Limited redundancy of the proprotein convertase furin in mouse liver. J Biol Chem 279:53442–53450
30. Spivak JL, Toretti D, Dickerman HW (1973) Effect of phenylhydrazine-induced hemolytic anemia on nuclear RNA polymerase activity of the mouse spleen. Blood 42:257–266
31. Zhang J, Socolovsky M, Gross AW, Lodish HF (2003) Role of Ras signaling in erythroid differentiation of mouse fetal liver cells: functional analysis by a flow cytometry-based novel culture system. Blood 102:3938–3946
32. Berube NG, Mangelsdorf M, Jagla M, Vanderluit J, Garrick D, Gibbons RJ, Higgs DR, Slack RS, Picketts DJ (2005) The chromatin-remodeling protein ATRX is critical for neuronal survival during corticogenesis. J Clin Invest 115:258–267
33. Palis J, Yoder MC (2001) Yolk-sac hematopoiesis: the first blood cells of mouse and man. Exp Hematol 29:927–936
34. McGrath KE, Koniski AD, Malik J, Palis J (2003) Circulation is established in a stepwise pattern in the mammalian embryo. Blood 101:1669–1676
35. McGrath KE, Palis J (2005) Hematopoiesis in the yolk sac: more than meets the eye. Exp Hematol 33:1021–1028
36. Higgs D, Wood WG (2005) Erythropoiesis. In: Hoffbrand AV, Catovsky D, Tuddenham EGD (eds) Postgraduate haematology. Blackwell, Oxford
37. Medvinsky A, Dzierzak E (1996) Definitive hematopoiesis is autonomously initiated by the AGM region. Cell 86:897–906
38. Muller AM, Medvinsky A, Strouboulis J, Grosveld F, Dzierzak E (1994) Development of hematopoietic stem cell activity in the mouse embryo. Immunity 1:291–301
39. de Bruijn MF, Speck NA, Peeters MC, Dzierzak E (2000) Definitive hematopoietic stem cells first develop within the major arterial regions of the mouse embryo. EMBO J 19:2465–2474
40. Schneider A, Zhang Y, Guan Y, Davis LS, Breyer MD (2003) Differential, inducible gene targeting in renal epithelia, vascular endothelium, and viscera of Mx1Cre mice. Am J Physiol Renal Physiol 284:F411–F417
41. McDowell TL, Gibbons RJ, Sutherland H, O'Rourke DM, Bickmore WA, Pombo A, Turley H, Gatter K, Picketts DJ, Buckle VJ, et al (1999) Localization of a putative transcriptional regulator (ATRX) at pericentromeric heterochromatin and the short arms of acrocentric chromosomes. Proc Natl Acad Sci USA 96:13983–13988
42. Berube NG, Smeenk CA, Picketts DJ (2000) Cell cycle-dependent phosphorylation of the ATRX protein correlates with changes in nuclear matrix and chromatin association. Hum Mol Genet 9:539–547
43. Nagy A, Rossant J (2001) Chimaeras and mosaics for dissecting complex mutant phenotypes. Int J Dev Biol 45:577–582
44. Rossant J, Spence A, Rossant J (1998) Chimeras and mosaics in mouse mutant analysis. Trends Genet 14:358–363
45. Tam PP, Rossant J (2003) Mouse embryonic chimeras: tools for studying mammalian development. Development 130: 6155–6163
46. Crosby JR, Seifert RA, Soriano P, Bowen-Pope DF (1998) Chimaeric analysis reveals role of Pdgf receptors in all muscle lineages. Nat Genet 18:385–388